DEVELOPMENT OF INTELLIGENT GAS-OIL FLOW PROCESS INTERPRETER BASED ON GENERIC PRIMARY ELECTRODE OF ELECTRICAL CAPACITANCE TOMOGRAPHY SENSOR

KHURSIAH ZAINAL MOKHTAR

UNIVERSITI SAINS MALAYSIA

2013

DEVELOPMENT OF INTELLIGENT GAS-OIL FLOW PROCESS INTERPRETER BASED ON GENERIC PRIMARY ELECTRODE OF ELECTRICAL CAPACITANCE TOMOGRAPHY SENSOR

by

KHURSIAH ZAINAL MOKHTAR

Thesis submitted in fulfilment of the requirements
for the degree of
Master of Science

May 2013

ACKNOWLEDGEMENTS

I especially wish to thank my supervisor, Associate Professor Dr. Junita Mohamad Saleh for her guidance during my research and study at the Universiti Sains Malaysia. Her perpetual energy and enthusiasm in research has motivated all her advisees including me. She has always been accessible and willing to help her students with their research. As a result, research life has become rewarding for me. She spent a lot of time correcting and proof-reading this thesis, which I very much appreciate.

I would also want to thank other lecturers who had taught me during my undergraduate study. May all their valuable knowledge and information help me to be a successful person.

I am also grateful to the Ministry of Science, Technology and Innovation (MOSTI), Malaysia for financially supporting this research under eScience fund grant No. 03-01-05-SF0134 and Ministry of Higher Education (MOHE), Malaysia for the Fundamental Research Grant Scheme, No. 203/PELECT/6071148.

My deepest gratitude goes to my family; my sister Dr. Annisa, her husband Akif Özyılmaz and her son Ali Iskender, little sister Munirah and much beloved little brother Cikgu Adnin and her wife, Cikgu Anisah for their unflagging love and support throughout my life; this dissertation is simply impossible without them. I am indebted to my father, Zainal Mokhtar Abdul Hamid, the first teacher of my educational career. Not forgetting, his love, sympathetic support, special prayers and best wishes. I am also very grateful for my stepmother, Sarimah Omar, without her continous support and encouragement I never would have achieved my goals.

I would also like to extend my deepest emotions, appreciation and love to all my friends; Najwan, Hafizah, Azian, Marlina, Norasyikin, Hosni, Eisha and Abdul Ghani and those who have hand-lifted to pray for me.

Finally, I dedicate this dissertation to the loving memories of my late mother, Ramlah Salleh.

TABLE OF CONTENTS

LIST OF TABLES

LIST OF FIGURES

LIST OF ABBREVIATIONS

ANN	Artificial Neural Network
AVGEF	Average Empty and Full
BP	Back Propagation
BR	Bayesian Regularisation
CCP	Correct Classification Percentage
CT	Computerised Tomography
DAS	Data Acquisition System
ECT	Electrical Capacitance Tomography
FE	Finite Element
GUI	Graphical User Interface
LBP	Linear Back Projection
LM	Levenberg-Marquadrt
Logsig	Logarithmic Sigmoidal
MAE	Mean Absolute Error
MINMAX	Minimum Maximum
MLFF	Multi-Layer Feed-Forward
MLP	Multi-Layer Perceptron
PC	Principal Component

PCA Principal Component Analysis

PT Process Tomography

QN Quasi-Newton

RAM Random Access Memory

SLFF Single-Layer Feed-Forward

SLMONN Single-Layer Multi-Output Neural Network

Tansig Hyperbolic Tangent Sigmoidal

SOM Self Organizing Map

WNN Wavelet Neural Network

PEMBANGUNAN PENTAFSIR CERDIK UNTUK ALIRAN GAS-MINYAK BERDASARKAN KEPADA ELEKTROD UTAMA GENERIK PENDERIA TOMOGRAFI KEMUATAN ELEKTRIK

ABSTRAK

Tomografi Kemuatan Elektrik (ECT) adalah teknik yang digunakan bagi mendapatkan maklumat taburan bahan-bahan dalam paip tertutup dengan cara mengukur variasi dalam sifat-sifat dielektrik taburan bahan-bahan tersebut. Beberapa penyelidikan ECT terdahulu telah dijalankan bagi mengklasifikasi rejim aliran dan menganggar pecahan bahan menggunakan kaedah Rangkaian Neural Buatan (ANN) yang hanya tertumpu kepada parameter penderia ECT yang tetap, lantas menghasilkan sistem-sistem pentafsir proses yang tidak cekap. Oleh itu, penyelidikan ini bertujuan membangunkan sistem pentafsir pintar yang dapat berfungsi untuk suatu julat nilai elektrod utama penderia ECT. Bagi tujuan ini, ANN Perceptron Berbilang Lapisan (MLP) telah dilatih dengan pelbagai set data ECT bagi tujuan menyiasat kaedah terbaik bagi menghasilkan pengelas regim aliran gas-minyak dan penganggar pecahan minyak pintar. Teknik Analisis Komponen Utama (PCA) juga digunakan untuk mengurangkan dimensi data masukan, mengurangkan masa latihan dan meningkatkan prestasi pengelas dan penganggar. Keputusan kajian menunjukkan pengelas gas-minyak pintar yang dibangunkan mampu memberikan purata ketepatan pengelasan sehingga 93.93% ke atas data ECT daripada elektrod utama generik. Nilai ketepatan ini adalah lebih tinggi daripada purata nilai ketepatan pengelasan daripada pengelas pintar yang dilatih dengan saiz elektrod utama yang tetap, iaitu 37.45% menggunakan set data ujian yang sama. Sistem penganggar pintar yang telah dibangunkan pula mampu menganggar pecahan minyak dengan ralat mutlak purata sebanyak 3.05%, bagi data ECT generik pelbagai jenis regim aliran. Nilai ralat ini adalah 3.25% lebih rendah berbanding ralat mutlak purata yang diperoleh oleh penganggar pecahan minyak pintar tidak generik yang terbaik, daripada set data ujian yang sama. Keputusan kajian yang memuaskan mendedahkan bahawa pencapaian pengelas dan penganggar pintar generik adalah lebih baik berbanding pengelas dan penganggar aliran tidak generik bagi tugasan mentafsir proses aliran.

DEVELOPMENT OF INTELLIGENT GAS-OIL FLOW PROCESS INTERPRETER BASED ON GENERIC PRIMARY ELECTRODE OF ELECTRICAL CAPACITANCE TOMOGRAPHY SENSOR

ABSTRACT

Electrical Capacitance Tomography (ECT) is a technique used to obtain information about the distribution of materials inside a vessel by measuring variations in the dielectric properties of the material distributions. Previous research works on ECT flow regime classification and material fraction estimation have employed Artificial Neural Networks (ANNs) approach focusing on fixed ECT sensor parameters, and hence producing inefficient process interpreter systems. Therefore, this research aims to develop intelligent process interpreter systems which function to accommodate a range of ECT primary electrode sensor sizes. For the purpose, Multilayer Perceptron (MLP) ANNs have been trained with different types of datasets to investigate the best method in producing generic intelligent gas-oil flow regime classifier and oil fraction estimator. The Principal Component Analysis (PCA) technique has also been used to reduce the dimensionality of input, reduce training time and improve the systems' performances. The developed intelligent gas-oil classifier has given 93.93% average correct classification accuracy from ECT data of generic primary electrode. This accuracy value is higher than the average classification accuracy of intelligent classifier trained with fixed ECT primary electrode size which is 37.45%, for the same test dataset. The developed intelligent oil fraction estimator has produced 3.05% mean absolute error (MAE) for generic ECT data of various flow regimes. This MAE is 3.25% lower than the MAE produced by the best non-generic intelligent oil fraction estimator, based on the same dataset. The satisfactory research results reveal that the performances of generic intelligent gas-oil classifier and oil fraction estimator are better than the non-generic gas-oil classifier and estimator for process interpretation tasks.

CHAPTER 1

INTRODUCTION

1.1 Background

In many industries, information on material flow such as flow regimes (Yan et al., 2004; Li-Feng and Hua-Xiang, 2008; Yu et al., 2010), vector velocity (Hayes et al., 1995; Xue et al., 2012), mass flow rate (Mosorov, 2008; Zheng and Liu, 2011) and component concentrations or material fraction (Wang, 2007; Wenli et al., 2007), are important process interpretation parameters to enact the safety and efficiency of industrial processes. These information are also useful for developing new process equipment and enhancing process operation. For instance, in oil production, information on flow regime inside a pipeline is essential as an indicator of overall oil production rate (Meglio et al., 2010). Meanwhile, information on material concentration or fraction, and velocity of flowing material is important in mining and environmental sectors as these could provide better understanding of corrosion and erosion effects in a pipeline (Bozzini et al., 2003). However, obtaining information for such process operation, control and safety within an oil pipeline is impossible and impractical due to concealed pipes. Also, insertion of normal sensors could disturb the flow of materials. Hence, Electrical Capacitance Tomography (ECT) which is a non-invasive method has been used to obtain various process measurements regarding multi-component flows in process equipment. ECT is a sensing technique suitable for concealed industrial processes involving non-conducting mixture such as gas-oil.

In ECT, several electrodes are mounted around a process equipment. These electrodes measure the changes in the capacitance between all possible pairs of electrodes with regard to various material distribution. From these measurements of capacitance differences, a cross-

sectional image can be reconstructed with the aid of an image reconstruction algorithm. In turn, intrepretation of process flow parameters can be determined from the cross-sectional image based on particular calculation and analysis. Figure 1.1 illustrates the ECT process interpretation work stages for obtaining information that is useful for process operation and control.

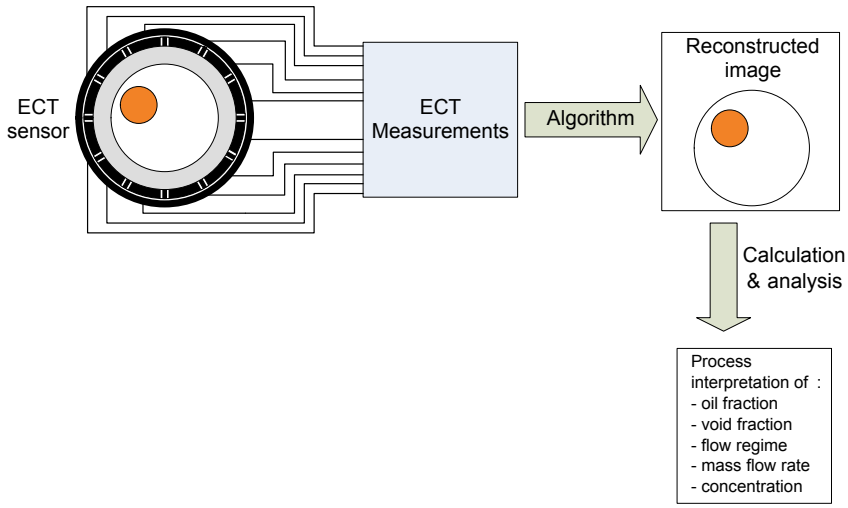

Figure 1.1: Process interpretation work stages

Image reconstruction is carried out using ECT image reconstruction algorithm. The Linear Back Projection (LBP) algorithm (Xie et al., 1989) was the first and simplest reconstruction algorithm ever proposed for ECT. However, images produced by LBP algorithm appear distorted due to the soft-field effect (Su et al., 2000). This fact has prompted many researchers to opt for different image reconstruction methods. The work by Nooralahiyan et al. (1994) was the first to show the capability of Artificial Neural Network (ANN) technique in reconstructing accurate tomographic images for different flow regimes from which, flow regime classification and void fraction were determined. Besides an ANN approach, a number of improved as well as new algorithms have also been introduced to obtain more accurate reconstructed images. These include the Landweber (Yang et al., 1999; Lu et al., 2005; Li and Yang, 2008) and Tikhonov algorithms (Lee et al., 2006; Lei et al., 2006; Jing et al., 2009). Although the advanced reconstruction methods have shown to be able to produce slightly more accurate images for some flow regimes, dis-

tortion of images is still a problem for few other regimes. Furthermore, the process of image reconstruction followed by process interpretation has been found to be time-consuming.

Image reconstruction method maybe tolerable for off-line works. Nevertheless, for on-line control and monitoring purposes, the approach is not suitable due to its long computational time. Hence, in some works, it is more appealing to utilise a direct process interpretation method. The work by Xie et al. (1992) was the first to employ a direct method for oil concentration estimation based on the average of normalised capacitance measurements. The method was simple and fast (i.e. did not require image reconstruction) but it was flow regime dependent in that different calibration methods were required for different flow regimes. Due to that, ANN method was then proposed as a method for direct process interpretation from ECT data (Mohamad-Saleh et al., 2001). The emergence of the method has been able to overcome the problems of soft-field effect, long process interpretation processing time and flow regime dependency. Since then, ANN has become a renowned artificial learning tool which is robust at solving numerous ECT-based problems. Its applications range from direct flow pattern recognition (Sun et al., 2002; Yan et al., 2004; Barbosa et al., 2010; Yu et al., 2010) to direct estimation of material fraction in pipelines without recourse to image reconstruction (Duggan and York, 1995; Williams and York, 1999; Mohamad-Saleh et al., 2001; Mohamad-Saleh and Hoyle, 2002). All these works have shown the superiority of ANN at direct process interpretation tasks based on ECT data.

1.2 Problems and Motivation

Despite the successes of works that employed ANN for direct ECT process interpretation, the intelligent system only worked for fixed ECT sensor parameters. The intelligent neural classifier and estimator were not generic in nature because they were trained with ECT data of fixed sensor parameter values. Mohamad-Saleh and Hoyle (2002) noticed that the employed ANNs were trained based on fixed ECT sensor parameters making them limited in "intelligence" and hence

they could not give more accurate process interpretation for data of different sensor parameter values. Therefore, it would be desirable to have an intelligent system which can accommodate a range of sensor parameter values.

In order to build a generic neural estimation system, various ECT parameters must be considered. Several previous works by Yan et al. (1999); Somerville et al. (1999), and Ahmed and Ismail (2008) had been carried out to analyse the sensitivity and resolution of the ECT sensor. The analyses have found that ECT primary electrode size plays an important role in influencing the sensing area sensitivity and resolution towards producing better tomograms. Reducing the size of primary sensors increases the resolution but decreases the sensitivity, and vice versa. From these findings, it can be deduced that a generic intelligent system can be developed by varying ECT primary electrode sizes. The main question is how to develop one. Therefore, an investigation on developing an intelligent generic process interpreter seems necessary.

1.3 Research Objectives

This research work aims to develop intelligent generic flow regime classifier and oil fraction estimator systems. As previous literature works have shown that primary electrode size is the most significant sensor parameter, this work focuses on genericity in terms of ECT primary electrode sizes. The objectives of the research are as follows:

(i) To develop an intelligent gas-oil flow regime classifier using ANN based on ECT data of various primary electrode sizes.

(ii) To develop an intelligent oil fraction estimator using ANN based on ECT data of various primary electrode sizes.

(iii) To assess the capability of the intelligent process interpreter systems at classifying gas-

oil flow regime and estimating oil fraction by comparing their performances with intelligent process interpreter trained with fixed-size primary electrode.

(iv) To design and implement a Graphical User Interface (GUI) for use with the developed intelligent classifier and estimator based on generic primary electrode.

In this research, a variant of Multi-Layer Feed-Forward (MLFF) ANN known as Multi-Layer Perceptron (MLP) has been used due its simple structure and its established capability at solving many ECT problems. All stages of the work have been carried out using the tools supported in MATLAB. The works have been done using a personal desktop computer having Core i7 (2.93 GHz) processor with 8 GB RAM.

1.4 Thesis Outline

This chapter introduces the research work. It briefs on the background, problems and motivation, objectives and the scope of the research.

Chapter 2 gives a brief overview of Electrical Capacitance Tomography (ECT), as it is the main subject of the research. Artificial Neural Networks (ANN) is also briefly reviewed. The training algorithms and activation functions used in this research are explained in this chapter. Then, a discussion on Principal Components Analysis (PCA) technique and its use in solving ECT problems are discussed.

Chapter 3 explains the methods employed towards developing intelligent classifier gas-oil and oil fraction estimator systems based on generic primary electrode. The proposed models for the tasks are first presented and briefly described. This is followed by explanation on the ECT sensor design used and how ECT data are collected. Then, the chapter explains how the proposed models are developed based on several investigations. The process of employing

the PCA is later explained. Finally the work stages involved in developing the Graphical User Interfaces (GUI) for use with the developed flow process interpretation systems are explained.

Chapter 4 presents the results of developed intelligent flow process interpretation systems. This includes discussion on the optimum number of training data, suitable normalisation method, the best baseline, the best training algorithm and the best activation function. The effects of PCA technique on the systems' performances and training times are also presented and discussed.

Chapter 5 gives a brief summary on the research work. This is followed by the conclusions of the investigation based on the obtained results. The final section of this chapter outlines the possible future works that can be carried out based on the foundation of this work.

CHAPTER 2

LITERATURE REVIEW

2.1 Introduction

This chapter briefly discusses Electrical Capacitance Tomography (ECT), one of the tomographic sensing techniques. The ECT sensor design and its general principles are addressed. This is followed by a discussion on Artificial Neural Network, and it then focusses on Multi-Layer Perceptron (MLP) which is used in this research. Next, discussion on flow regime classification and oil fraction estimation are presented. Finally, an overview of Principal Component Analysis (PCA) method for obtaining the uncorrelated input components is explained.

2.2 Electrical Capacitance Tomography (ECT)

The origin of the word "tomography" is from Greek words; “tomos” meaning slice or section and “graphe” meaning drawing. Tomographic measurement technique was first applied to medical imaging in 1970s. A Computerised Tomography (CT) machine uses radiation source (such as x-ray or γ-ray) that rotates around a human body to obtain a set of measurements. These measured data are used to reconstruct a cross-section of the human body.

In the 1980s, tomographic technique was introduced for industrial processes. Known as Process Tomography (PT), it has become increasingly popular with its adoption and implementation based on various modalities and techniques. However, the most conspicuous PT techniques are those based on measurement of electrical properties through utilization of capacitive, conductive, or inductive nature of materials under investigation. Of these electrical tomographic techniques,

capacitance tomography is in the most advanced state of research and development for industrial process applications. Electrical Capacitance Tomography (ECT) is a sensing system which uses capacitive measuring technique. It normally consists of copper electrode plate sensors which are sensitive to differing dielectric constants of materials. The sensors are mounted equidistantly around the periphery of an insulating process equipment at a point of interest. Different materials have different values of dielectric constants also known as relative permittivities. Hence, the distribution of two-component flows within an ECT sensing region produces a change in the capacitance measurements between two electrodes. The effective capacitance that occur between pairs of electrodes inside a pipe vessel are measured. Then, an appropriate image reconstruction algorithm is used to reconstruct an image of such material distribution using the capacitance measurements. The tomographic images obtained from the imaging process are not only useful in determining the flow regime but also the vector velocity and component concentration in process vessels and pipelines. ECT has been applied in various industrial control operations such as imaging of two-component flow of gas-oil in pipelines (Wang, 2007; Ahmed and Ismail, 2008), gas-solid flows in pneumatic conveyer (Arko et al., 1999; Mosorov, 2008; Zheng and Liu, 2011) and separation of oil, water and gas in plant vessel (Bukhari and Yang, 2006; Jaworski and Meng, 2009).

Figure 2.1 illustrates an ECT system consisting of the sensor system, the data acquisition system (DAS) and the computer system. The sensors produce differential voltage between all possible electrode combinations. These measurements are taken by the DAS which is also responsible for converting the ECT measurements into digital signal and sending the signal to the computer system. The computer has two main functions. First, it controls the measurement operations performed by the DAS through the sensors. Second, by means of an appropriate algorithm, it uses the measured capacitance data to produce useful information represented either qualitatively in the form of a reconstructed image of flow process and/or quantitatively in

the form of flow parameter estimations.

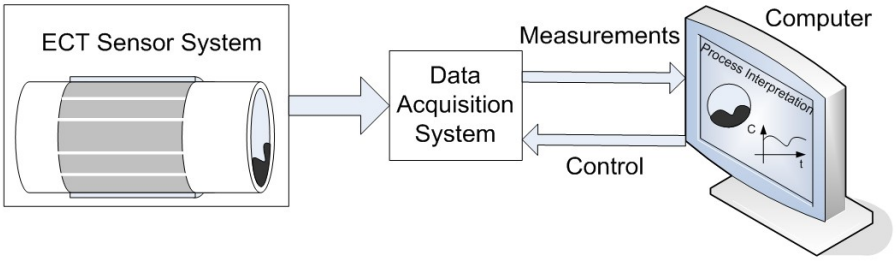

Figure 2.1: A schematic diagram of an ECT system

2.2.1 ECT Sensor Design and Parameters

Basically, an ECT sensor consists of primary electrodes, guard electrodes and an outer screen as shown in Figure 2.2. Figure 2.3 gives an illustration on typical ECT sensor design and parameters for an oil pipeline. From the figure, R_1 is the inner radius within the sensing region.R_2 is the outer radius which extends from the middle point of a pipe to the ECT sensor system.R_3 is the radius of electrode screen which shields the whole sensor system. The primary electrode angular size, θ is one of the important parameters affecting the system's sensitivity. The guard electrode size, β most often depends on the size of θ. The sizes of these parameters play important role in an ECT system (Yang, 2010; Mohamad et al., 2011).

The primary electrodes are used to accumulate charges to generate electric field in order to create capacitance effect to measure capacitance values. The outer screen placed around the electrodes shields the sensor system from the effects of extraneous variations in the stray capacitance to earth. Stray capacitance is an undesirable capacitance that usually occurs within the CMOS switches in the measuring circuit, within the cables connecting the electrodes to the measuring circuits and the sensor screen (Yang, 1995). The earthed guard electrodes placed between adjacent primary electrodes are used to reduce the standing capacitance between adjacent electrodes. They are also used to confine the electric field lines within the pipe regions

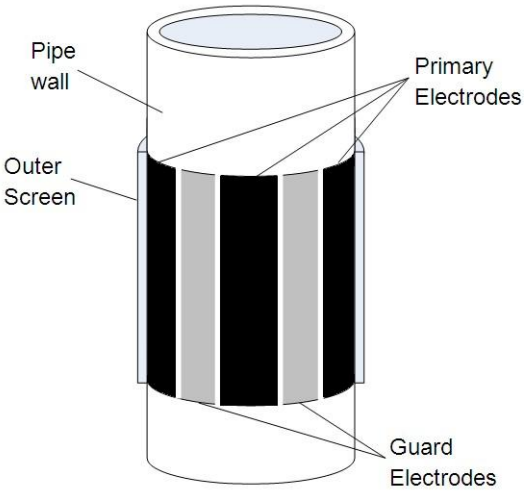

Figure 2.2: A 3-D schematic of ECT sensor array

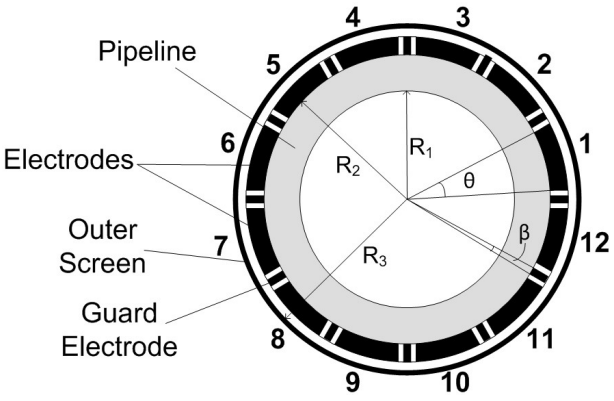

Figure 2.3: A typical 2-D schematic diagram of an ECT sensor model attached around a pipeline (adapted from Mohamad-Saleh and Hoyle, 2002)

referred to as positive sensing area. Thus, the electric field lines cannot travel between adjacent primary electrodes as shown in Figure 2.4.

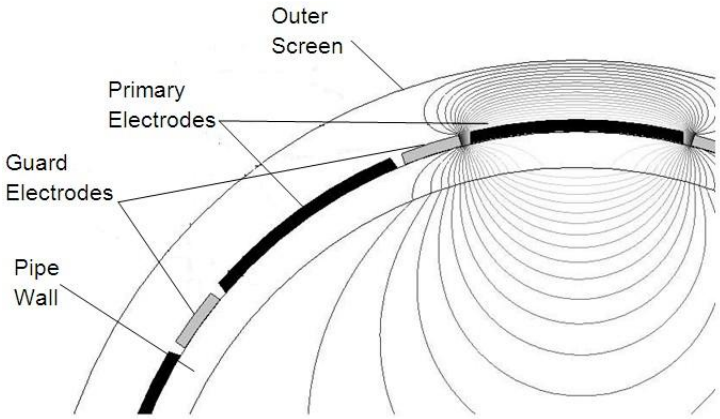

Figure 2.4: Electric field lines being confined by the earthed guarding electrodes (adapted from Martinez et al., 2006)

As illustrated in Figure 2.4, the field lines traveling from the source electrode through the pipe wall, crossing the equi-potential lines vertically, die at the grounded guard electrode before they can reach the adjacent electrode. The external field lines are neutralised by the grounded outer screen. Consequently, the capacitance measured between these electrodes is due only to the field lines that cross the region under study (i.e. the interior of the pipe).

A vital step in planning a successful ECT application is the design of the capacitance sensor unit. Various design parameters of ECT sensors interact and affect the overall sensor performance and various design rules (Yan et al., 1999; Alme and Mylvaganam, 2006; Yang, 2010) have been developed which allow an effective ECT sensor to be constructed for a specific application. For instance, the number and the size of measuring electrodes are two design parameters of a sensor unit which are application dependant. With the increase in the number of electrodes, the number of independent measurements increases and a higher resolution image can be obtained. However, too many electrodes results in smaller electrode size which leads to lower measurement sensitivity compared to a sensor unit with fewer electrodes. Sensitivity can be

increased by using bigger electrodes though this will decrease resolution and therefore, a good image cannot be obtained.

Until now, most applications have used ECT sensors with 8, 12 or 16 electrodes (Flores et al., 2005). Currently, 8 or 12 electrodes are commonly used in an ECT sensor for various applications. This is because the number is a good compromise between sensitivity and resolution. Six and 16 electrodes are less commonly used in applications. Table 2.1 summarises the use of different numbers of electrodes in various applications.

Table 2.1: Example applications of ECT sensors with various number of electrodes and their application

Number of electrodes	Application
6	Visualising combustion flame in an engine cylinder with an attempt to achieve 36000 frames per second (Waterfall et al., 1996) Imaging of gas-water flows (Worasawate and Klongpramong, 2007) Monitoring high-shear mixing and high-shear granulation processes (Rimpilainen et al., 2011)
8	Imaging wet gas separator (Yang et al., 2004) Imaging oil-water flows (Chen et al., 2008) Imaging gas-solid flows in horizontal pipe (Daoye et al., 2009)
12	Measuring gas-oil-water three components flows (Ismail et al., 2005) Imaging of shallow bubble columns in air-kerosene mixture (Al-Masry et al., 2010) Imaging pharmaceutical fluidized beds (Wang and Yang, 2011) Measuring void fraction in an air-water co-current bubble column (Ismail et al., 2011)
16	Estimating metal fill profile in lost foam casting (Deabes et al., 2008) Imaging of processes in a bubble column (Smolik, 2010) Imaging water and dicholoromethane droplets of low concentration in the encapsulation chamber (Rezvanpour et al., 2012)

2.2.2 General Principles of ECT Measurement

ECT systems are used to measure permittivity distribution of pipe contents by measuring the inter-electrode capacitances. ECT systems work well for a two-component system, which is modeled as a combination of two substances having different relative permittivities. For an ECT

system, air has a relative permittivity of 1. Assuming the other component have a dielectric constant ε_k, the capacitance between any two electrodes is given by (Alexander and Sadiku, 2012)

$$C = \frac{A\varepsilon_0\varepsilon_r}{d} \tag{2.1}$$

where A is the area of electrode cross-section, ε_0 is the permittivity of free space and *d* is the distance between the electrodes. The dielectric constant ε_r is the relative permittivity.

Each time measurement is made, one of the primary electrodes acts as an excited electrode (an electrode which is excited at a potential voltage) and the remaining electrodes become the sensing electrodes (held at the potential ground). For instance, for a 12-electrode ECT sensor, if electrode 1 is the excited electrode, all other 11 electrodes become the sensing electrodes. As such, measurement protocol in the data acquisition system first measures the difference in capacitance between electrodes 1 and 2 ($C_{1,2}$), then between electrodes 1 and 3 ($C_{1,3}$), and so forth up to 1 and 12 ($C_{1,12}$). Then, the measurement procedures continue with the differences in capacitance between electrodes 2 and 3 ($C_{2,3}$), and so forth up to 2 and 12 ($C_{2,12}$). These measurements continue until the differences between all possible pairs of electrodes are measured. The excited electrodes and the capacitance measurements produced are shown in Table 2.2.

Table 2.2: Capacitance measurements produced from pairs of excited and other electrodes, which form a set of ECT data for a flow

Excited Electrode	Pairs of Capacitance Measurements
1	$C_{1,2}$ $C_{1,3}$ $C_{1,4}$ $C_{1,5}$ $C_{1,6}$ $C_{1,7}$ $C_{1,8}$ $C_{1,9}$ $C_{1,10}$ $C_{1,11}$ $C_{1,12}$
2	$C_{2,3}$ $C_{2,4}$ $C_{2,5}$ $C_{2,6}$ $C_{2,7}$ $C_{2,8}$ $C_{2,9}$ $C_{2,10}$ $C_{2,11}$ $C_{2,12}$
3	$C_{3,4}$ $C_{3,5}$ $C_{3,6}$ $C_{3,7}$ $C_{3,8}$ $C_{3,9}$ $C_{3,10}$ $C_{3,11}$ $C_{3,12}$
4	$C_{4,5}$ $C_{4,6}$ $C_{4,7}$ $C_{4,8}$ $C_{4,9}$ $C_{4,10}$ $C_{4,11}$ $C_{4,12}$
5	$C_{5,6}$ $C_{5,7}$ $C_{5,8}$ $C_{5,9}$ $C_{5,10}$ $C_{5,11}$ $C_{5,12}$
6	$C_{6,7}$ $C_{6,8}$ $C_{6,9}$ $C_{6,10}$ $C_{6,11}$ $C_{6,12}$
7	$C_{7,8}$ $C_{7,9}$ $C_{7,10}$ $C_{7,11}$ $C_{7,12}$
8	$C_{8,9}$ $C_{8,10}$ $C_{8,11}$ $C_{8,12}$
9	$C_{9,10}$ $C_{9,11}$ $C_{9,12}$
10	$C_{10,11}$ $C_{10,12}$
11	$C_{11,12}$

The total number of capacitance measurements *N* can be calculated using (Alme and Mylvaganam, 2006)

$$N = \frac{n(n-1)}{2} \tag{2.2}$$

where *n* is the number of electrodes used in an ECT sensor system. Therefore, for a 12-electrode sensor, there are 66 possible values of inter-electrode capacitances.

2.2.3 ECT Data Normalisation Model

The relation between two sensing electrodes can be linear or nonlinear in nature depending on the normalisation models; series or parallel, used to characterise the way in which the contents occur (Yang and Byars, 1999; Dong and Guo, 2008). From equation (2.1), it can be seen that the capacitance measured depends on the relative permittivity of the materials, the size of electrodes and the distance between two electrodes. However, it is an undeniable fact that the electrode capacitances are also strongly depend on the electrodes geometric configuration whereby the capacitance responses between different electrode combinations present a great distinction in magnitude and distribution profile. In order to eliminate the effect and reduce systematic errors in the measurement system, the measured capacitances need to be normalised either based on a series or parallel model. Both models treat each pair of measuring electrodes as an ideal parallel-plate capacitance sensor (Dong and Guo, 2008) and assume that the distribution of the two types of materials is in parallel or series arrangement. Figure 2.5 shows a parallel-plate capacitor with c_1 and c_2 representing the thickness (i.e. volume fraction) of the high permittivity material for parallel and series models, respectively.

For the parallel model shown in Figure 2.5(c), the measured capacitance between electrode pair *i-j* can be expressed as the sum of the two capacitances:

$$C_{i,j} = (1-c_1)C^l_{i,j} + c_1 C^h_{i,j} \tag{2.3}$$

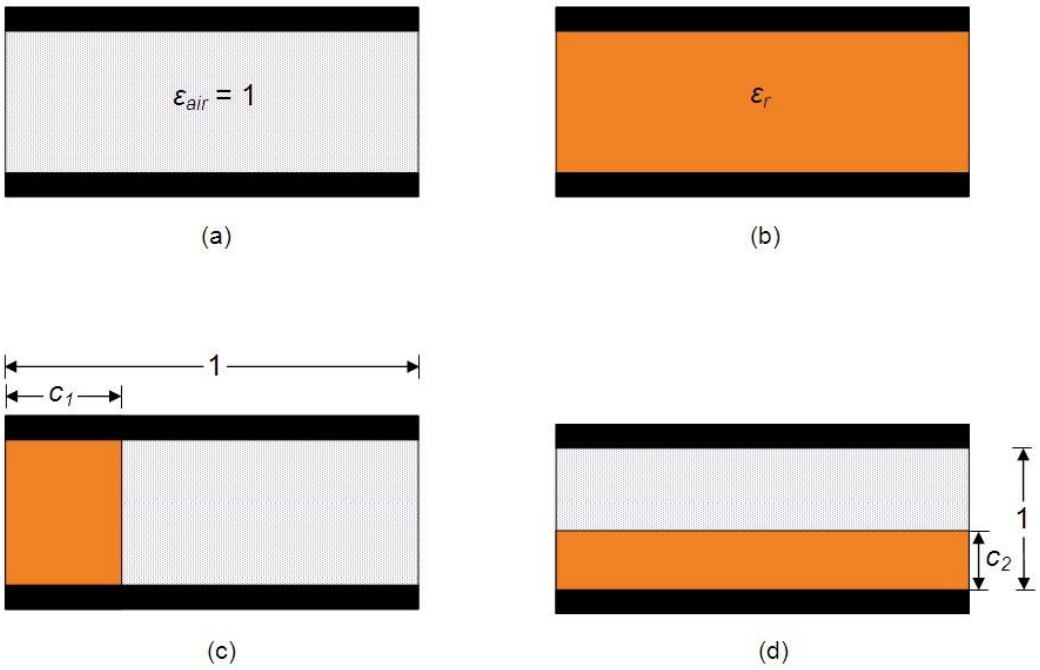

Figure 2.5: Schematic diagram of ECT sensor cross-section of (a) an emptied pipe (b) a pipe filled with highly permittivity material (c) parallel model, and (d) series model

where C^l is the capacitance of lower permittivity material and C^h is the capacitance of higher permittivity material.

For series model, it is given by

$$\frac{1}{C_{i,j}} = \frac{1-c_2}{C^l_{i,j}} + \frac{c_2}{C^h_{i,j}} \tag{2.4}$$

Rearranging equations (2.3) and (2.4), the parallel and series normalised capacitances $C^1_{i,j}$ and $C^2_{i,j}$ can be obtained as (2.5) and (2.6), respectively,

$$C^1_{i,j} = \frac{c_{i,j} - c^l_{i,j}}{c^h_{i,j} - c^l_{i,j}} \tag{2.5}$$

$$C^2_{i,j} = \frac{\frac{1}{c_{i,j}} - \frac{1}{c^l_{i,j}}}{\frac{1}{c^h_{i,j}} - \frac{1}{c^l_{i,j}}} \tag{2.6}$$

Equation (2.5) is also referred to as the conventional normalisation (Xie et al., 1992) whereby the normalised capacitance is a linear function of the measured capacitance in contrast to the series normalised capacitance being a nonlinear function (Yang and Byars, 1999).

2.3 Artificial Neural Network

Human's brain ability to make decision in solving very complex tasks, which are difficult for the conventional step-by-step computer programming method to solve, has led to the development of artificial neural network (ANN). ANN has been widely accepted and become a successful computational elements due to its advantages over the conventional algorithms. ANN has the ability to represent any simple or complex, and linear or nonlinear functions; that it is also called universal approximator (Kim et al., 2011). In addition, ANN is also more fault-tolerant than other algorithms because small changes in the input values normally cause no changes in the output values at all. The fault tolerance also allows ANN to adapt to failure of single or multiple neurons due to its information-distribution characteristic. This allows the whole system to still be efficient enough although some neurons fail (Sifaoui et al., 2008; Anastassiou, 2011). Furthermore, due to its massive network structure and inherently parallel nature, very high computational rate can be achieved when ANN is implemented directly into hardware or simulated using parallel algorithm (Yammenavar et al., 2011). Due to these reasons, ANN has been applied in wide ranging areas of human interests including medicine (Ecke et al., 2012), business and finance (Falavigna, 2012), robotic control (Kimn et al., 2012), signal processing (Yang et al., 2012), data processing (Sun et al., 2012) and non-linear control (Wahab et al., 2011).

An artificial neuron is a mathematical function conceived as a crude model of biological neuron. Figure 2.6 shows a basic model of artificial neuron. The computational element is often called a unit or node. The node receives input from some other nodes or from an external source. Each input x has an associated weight w that can be modified which corresponds to the

brain learning through the modification of the chemical information through the synapses. The node calculate some function *f* of the weighted sum of its input:

$$y_i = f(\sum_{j=1}^{n} w_{ij} y_j) \tag{2.7}$$

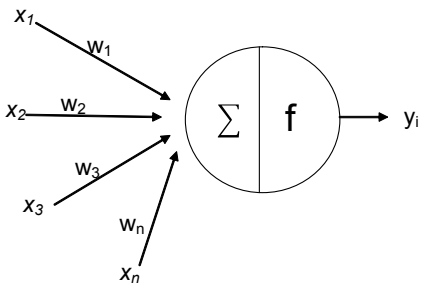

Figure 2.6: Artificial neuron

The weighted sum $\sum_j w_{ij} y_j$ is called the net input while the function *f* is the node's activation function. y_i is the output of the node which in turn can serve as input to other nodes.

An ANN can be classified by the type of learning scheme; either supervised or unsupervised. Each learning scheme can be categorised into its architectural types. Supervised learning involves training ANN by providing it with inputs and matching output patterns. Unlike the supervised learning, unsupervised learning, involves presenting an ANN with only inputs. The system must then develop its own representation of the input stimuli. Unsupervised learning has been reported to be less efficient at classification and approximation tasks (Saboori et al., 2010). This work adopts supervised learning and hence only this learning scheme is discussed.

Basically, there are three types of supervised ANN architectures; Single-Layer Feed-Forward (SLFF), Multi-Layer Feed-Forward (MLFF) and recurrent. SLFF is a linear ANN which can only solve linear problems. MLFF is one of the universal approximators, capable of solving linear and

non-linear problems. Recurrent ANN is similar to the MLFF with more complex structural links, and hence may be more computation-intensive. This work considered the use of MLFF ANN.

2.3.1 MLP Structure

MLP is a variant of the supervised MLFF. It has simple structure and hence it is fast, but yet capable of solving most nonlinear problems. Classification and estimation are among the most successful applications that have been solved with MLP (Pham et al., 2012; Mirjalili and Sadiq, 2011).

The basic architecture of MLP consists of three types of neuronal layer: input, hidden and output. Figure 2.7 shows a three-layer feedforward MLP. Each layer consists of neurons which

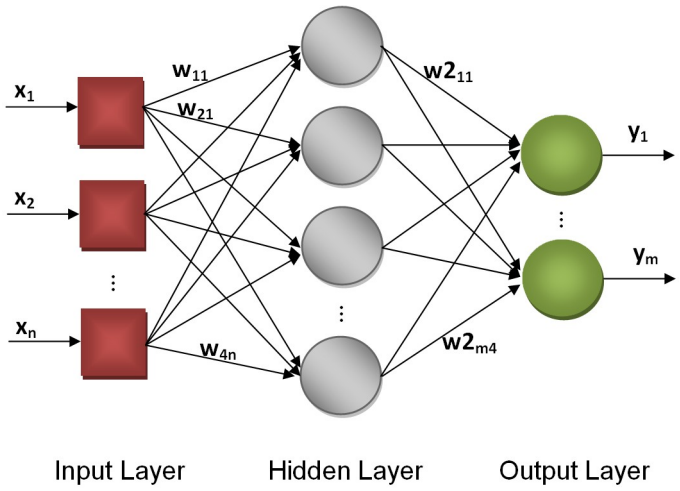

Figure 2.7: A schematic diagram of Multi-Layer Perceptron (MLP) for neural network (adapted from Saboori et al., 2010)

act as the processing elements. Input signals, $x_1, x_2, \ldots, x_n$ are fed to an MLP via its input neurons. Then, these input neurons pass the signals to the hidden neurons via the input weight connections, $w_{11}, w_{21}, \ldots, w_{4n}$. The hidden neurons execute some computations and transmit the results to the output neurons via the output weight connections, $w2_{11}, w2_{21}, \ldots, w2_{m4}$. The output neurons then carry out further computation and present the final results, $y_1, \ldots, y_m$. The

number of input, hidden and output neurons in a MLP is problem dependent. The number of input neurons usually corresponds to the number of available measurements or parameters related to a problem. The number of output neurons correspond to the number of solutions required. For example, in a classification problem, the number of output neurons equal the number of classes involved. The number of hidden neurons for solving a task is to be determined. Determining the optimum number of hidden neurons in an MLP is very crucial. An MLP with too few hidden neurons will not have enough capability to represent the input-output mapping. An MLP with too many hidden neurons on the other hand, leads to a problem of data over-fitting where the MLP simply memorises the training data and ends-up with a poor generalisation capability.

2.3.2 MLP Learning

Training of a MLP involves adjustment of its weights to match the actual outputs to desired outputs of the MLP. A weight specifies how strong a connection is between two artificial neurons. Usually, initial MLP weights are simply set to small random numbers and they can be positive or negative values. This provide the training algorithms with a good starting point to work towards a solution. Hence, as a MLP training process proceeds its weights are adjusted to produce accurate results to an associated.

An activation function, which is also known as threshold function or transfer function, is a function that described the output behaviour of a neuron (Karlik and Olgac, 2011). It is used to limit the output amplitude of a neuron to some finite or bounded value. The choice of activation function is important for the performance of a training algorithm towards achieving good output accuracy. Some of the most commonly used activation functions to solve non-linear problems using MLP are the logarithmic sigmoidal and hyperbolic tangent sigmoidal (Dixit and Dixit, 2008; Isa et al., 2010).

Figure 2.8 shows the logarithmic sigmoidal function which saturates to either near 0 or 1. These two values are used to indicate the membership of an output class. The expression for this function is given by

$$f(x) = \frac{1}{1+e^{-kx}} \tag{2.8}$$

where x is the sum of weighted inputs and k is the slope constant commonly set to 1. The input x for this function varies from $-\infty$ to $+\infty$. The output is within (0,1).

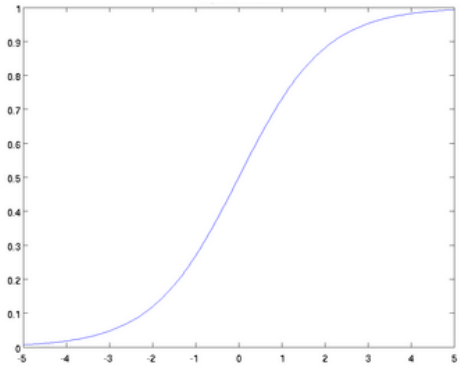

Figure 2.8: Logarithmic sigmoidal activation function

Another most common activation function used in MLP is the hyperbolic tangent sigmoidal activation function. This function is similar to the logarithmic sigmoidal activation function in transforming the net weighted input to saturate output class to between -1 and +1. Figure 2.9 shows the plot of this function and the expression is

$$f(x) = \frac{1-e^{-kx}}{1+e^{-kx}} \tag{2.9}$$

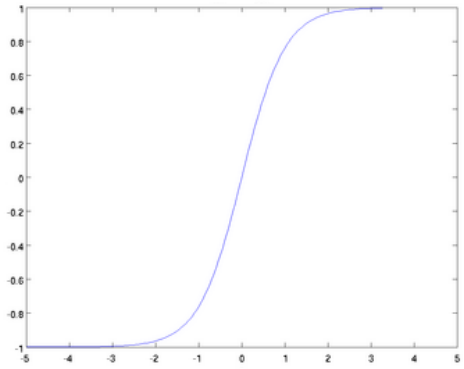

Figure 2.9: Hyperbolic tangent sigmoidal activation function

2.3.3 MLP Training Algorithm

The Back Propagation (BP) algorithm is a preferred algorithm used to train a MLP. Its original version was proposed as early as 1960s (Rosenblatt, 1962) and later improved by Werbos (1974); Parker (1982) and finally by Rumelhart and McClelland (1982).

Not-withstanding its popularity, the traditional BP algorithm, which uses the Gradient Steepest Decent mehod suffers from two major shortcomings; it converges slowly to the optimal solution and it may yield a poor solution as it can be trapped at a locally optimised solution. This algorithm is obviously too slow for a practical problem and hence several researches on methods to accelerate its learning process have been carried out.

The faster algorithms can be divided into two categories. The first one uses heuristic methods which involves optimising various BP algorithms parameters such as varying the learning rate, using momentum and rescaling the variables as well as BP's topology. Although the modifications of these two aspects significantly influence the speed towards achieving a solution, they do not guarantee convergence towards a globally optimal solution.

The second category of fast BP algorithms adopts stochastic numerical optimisation techniques. These techniques include the Conjugate Gradient, Quasi-Newton and Levenberg-Marquardt

methods. Conjugate Gradient methods are rarely used as a primary method to solve various problems because they require time-consuming line search method (Butt, 2009). MLP training is normally considerably faster when Quasi-Newton (QN) and Levenberg-Marquardt (LM) are utilised but they tend to be less efficient for MLP training with several thousand of weights. This is because they require more memory and longer computation time (Demuth and Beale, 2010). Nevertheless, problems involving thousands of weights are rare. The LM algorithm has been a commonly used training method for various applications (Khajeh et al., 2012; Keçebaş and Yabanova, 2012; Nadimi et al., 2012; Kana et al., 2012; Aghbashlo et al., 2012).

Bayesian Regulation (BR) training algorithm is an extended or modified version of LM training algorithm. Although, this training algorithm updates weight and bias values according to LM optimisation, it has a different performance function from the LM training algorithm. The difference being that it minimises MLP error along with the weights and biases. Then, it determines the best combination so as to produce a network that generalise well (Thakare and Singhal, 2011). This method has shown its capability to produce MLP with smaller and smoother weights and biases that over-fitting of training data can be prevented (Ni et al., 2009; Chamjangali and Ashrafi, 2013).

The process of selecting the best training algorithm depends on the nature of a problem. To select an efficient training algorithm for a certain problem, a number of training runs are performed using different training algorithms. Then, the best one is chosen based on the best-performed MLP. The work involves extensive MLP training runs.

2.4 ECT Process Interpretation

In ECT, the changes in the capacitance between all possible combinations of electrodes are measured when dielectric materials such as a mixture of oil and gas is introduced into the sensing region of process equipment. From these capacitance measurements, an image based on the

variation of material permittivity within a cross-section can be obtained using sophisticated algorithms. The images are analysed to compute and interpret the parameters related to the process such as spatial distribution, volume ratios of fractions of the materials, types of flows (i.e. flow regime) and the velocities of the flow inside the pipe. This process is referred to as process interpretation.

2.4.1 ECT Flow Regime Classification

Classification, which is the task of assigning objects to one of several predefined categories, is a pervasive problem that encompasses many diverse applications. This type of information is certainly useful in numerous industrial applications such as petroleum extraction and processing, nuclear power plant and various chemical reactors. It is also one of the most important subject to enact the efficiency and safety in aggressively fast-moving fluids in multiphase mixture in a process equipment (Zong et al., 2010). Although there various techniques can be employed to identify flow regimes, ECT measuring technique is a highly attractive technique due to its capability at obtaining measurements non-invasively, non-intrusively and with no radiation involved, unlike other conventional technique.

Two methods that can be adopted for the task of process interpretation; ECT image reconstruction and direct methods. A cross-sectional image can be reconstructed using ECT data with an aid of an image reconstruction algorithm. Meanwhile, the direct method is a rather straightforward method of classifying flow regime using the capacitance measurements based on some statistical manipulation or intelligent system.

The classification of flow regimes using an image reconstruction algorithm was first developed by Xie et al. (1989). However, images produced by the algorithm appear distorted due to the soft-field effect. Later many other more robust image reconstruction methods such as Landweber,

Tikhonov and iteration methods have been proposed, but with few other associated problems particularly flow regime dependent (Mohamad-Saleh et al., 2001). This fact has prompted many researchers to opt for different reconstruction methods to overcome the problems associated with the conventional image reconstruction algorithms.

In 1994, Nooralahiyan et al. (1994) was the first to carry out work on flow regime identification using ANN replacing the conventional image reconstruction algorithms. Based on an 8-electrode ECT system, a Single Layer Multi-Output ANN (SLMONN) with 28 input neurons (corresponding to 28 capacitance measurements) fully connected to a grid of 100 neurons in the output layer (corresponding to the spatial image) was developed. The SLOMNN was trained to learn different features of four different flow regimes (i.e. bubble, core, annular and stratified flows) to their respective output patterns. Given a set of capacitance measurements and superimposing the associated output patterns, the SLMONN learned to construct tomographic images by extracting features and mapping them onto the 100 grids of neurons. The results showed that ANN produced more accurate tomograms compared to the conventional image reconstruction algorithms. However, the process of image reconstruction is very time-consuming, hence direct method have been employed by many researchers to get fast results.

In a research by Sun et al. (2002), ECT data in a form of differential pressure signal was processed using wavelet analysis to extract six significant features. Then, a Multi-Layer Perceptron (MLP) ANN model was employed to learn the features and classify four different flow regimes, namely annular, bubble, plug and slug flows. The correct flow regime identification percentage obtained was 86.76%. Yan et al. (2004) presented ten features extracted from ECT measurements to a MLP ANN and trained them to classify eight different flow regimes. The MLP attained an average of 93.7% correct identification percentage. Barbosa et al. (2010) studied flow regime identification gas-solid and gas-liquid using a Self Organizing Map (SOM) neural network. The data used not only contain ECT measurements but also values of pressure drop and fluctuating